A Methodological Development of Accessing Greenness Visibility from Open-Source Street View Images: A Multi-City and Multi-Country Implementation

Ilse Abril Vázquez Sánchez

2016362

Supervised by:

Dr. S.M. Labib (Utrecht University)

A dissertation submitted in partial fulfillment of the requirements for the degree of

Master of Science in Applied Data Science

Utrecht University

June 2023

Acknowledgement

I wish to extend my deepest appreciation to my family back in Mexico who have tirelessly supported me throughout my studies in the Netherlands. This thesis represents not only my personal achievement but also stands as a testament to the persistent support of my family back home.

First and foremost, I am profoundly grateful to my loving parents. Despite the physical distance between us, I feel your presence in my life every single day. Your support has been the cornerstone of my success, and I will forever cherish your unconditional love, encouragement, and guidance. As I continue this journey, embracing new challenges and opportunities, I promise to honour your sacrifices and make you proud by working diligently and making the most of the education I am privileged to receive.

To my treasured sister, I want to express my heartfelt gratitude for being my guiding light and constant source of inspiration. From the moment I embarked on this adventure, you have been by my side, offering guidance, encouragement, and love. Your presence in my life has shaped me into the person I am today, reminding me of the importance of perseverance, passion, and kindness.

Furthermore, to the dear friends I have made in the Netherlands. Your friendship has provided invaluable support and has made this life-changing experience much easier for me. Thank you for brining different cultures, perspectives, and experiences into my life. Your presence has not only made the Netherlands feel like a home away from home but also has created a diverse and vibrant community that transcends geographical boundaries.

Also, I would like to sincerely thank Dr. SM Labib for his exceptional guidance throughout the realisation of this project. From the very beginning, you have shown immense passion and commitment to the project, motivating me to explore new ideas and challenging me to achieve my best. Your passion for research and your dedication to fostering academic excellence have been truly inspiring. I am grateful for the opportunity to have worked under your guidance, and I will carry the skills and knowledge gained through this experience with me during my academic and professional journey.

Lastly, I would like to wholeheartedly express my deep appreciation to Utrecht University for awarding me the Utrecht Excellence Scholarship. The scholarship not only played a crucial role in making my dream of studying Data Science a reality but also broadened my perspectives and equipped me with the necessary tools to make a positive impact in this field. I am committed to honouring the trust and investment placed in me by striving for academic excellence, making a positive impact in society, and contributing to the university's legacy.

Abstract

Urban green spaces provide numerous benefits, including augmenting the aesthetic appeal of urban landscapes and improving mental wellbeing. While diverse methods have been used to evaluate greenery, the assessment of green visibility using street-view level images is frequently recommended due to its greater compatibility with human perception. Although many existing studies predominantly rely on Google Street View data, the usage restrictions and lack of alignment with FAIR (Findability, Accessibility, Interoperability and Reusability) principles presents challenges. Therefore, the incorporation of Volunteered Street View Imagery (VSVI) platforms, such as Mapillary, is emerging as a promising alternative. This research presents a scalable and reproducible framework for assessing the Green View Index (GVI) using Mapillary data in diverse global urban contexts. By documenting a step-by-step procedure encompassing data acquisition, image segmentation, and GVI calculation, this study ensures the accuracy and consistency of future analyses. To address the research questions, the study examines the variations in image availability and usability of Mapillary data for green view assessments across different cities worldwide. The findings reveal significant disparities in open-source image availability, highlighting cities with high image availability in the USA and Europe, as well as cities with limited availability located in Africa and South Asia. Furthermore, the study evaluates the suitability of using Normalised Difference Vegetation Index (NDVI) values to fill in missing data points in GVI assessments. The analysis demonstrates that the NDVI can effectively calibrate a Linear Regression model to estimate GVI values, even in regions where street-view imagery is limited. Additionally, the analysis reveals notable disparities in GVI across cities, particularly in high-density, lower-income cities in Africa and South Asia compared to low-density, high-income cities in the USA and Europe.

Table of Contents

1. Introduction

Green spaces play a crucial role in urban environments, offering a wide array of social, environmental, and ecological benefits (Bain et al., 2012; Gómez-Baggethun & Barton, 2013; Ordóñez et al., 2023; Saw et al., 2015). As the urban population is projected to increase by 60% by 2050 (United Nations, 2018), sustainable development becomes imperative in addressing pressing issues including climate change mitigation and improving the quality of life for urban residents (Savo et al., 2023). Urban green spaces provide multifunctionality to enhancing the environmental quality within cities. They effectively mitigate the heat island effect (Keeley, 2011; Lafortezza et al., 2009), improve air quality by reducing pollutants (Akbari et al., 2001; Jim & Chen, 2008), reduce noise pollution (Attal et al., 2021; Wong et al., 2010), and minimise stormwater runoff (Armson et al., 2013; Berland et al., 2017). Moreover, the visual perception of street greenery is recognised as a vital sensory function that positively influences individuals' experiences in urban settings (Lu et al., 2018; Wolf, 2005). Urban greenery serves as a protective barrier against visual intrusion (Li, Zhang, Li, Kuzovkina, et al., 2015). Furthermore, the presence of vegetation in urban landscapes often leads to higher aesthetic ratings of streetscapes (Lindemann-Matthies & Brieger, 2016), promoting physical activities (Zijlema et al., 2020) and fostering social cohesion among residents (Root et al., 2017). From a health perspective, visual contact with greenery evokes positive emotions, reduces stress, and facilitates the recovery of mental fatigue (Kaplan, 1995; Ulrich, 1984; Wang et al., 2022).

Different assessment methods have been employed to measure and evaluate urban greenery, including surveys, interviews, and audits, to gain insights into people's opinions and attitudes towards street-level views of urban greenery (Falfán et al., 2018; Li, Zhang, Li, Ricard, et al., 2015). However, each of these methods have its advantages and limitations. Surveys using questionnaires may be more reflective of people's personal experience on the ground but may be affected by response bias. (Downs & Stea, 1977). Additionally, audits require skilled evaluators and specific criteria to assess visual aesthetic quality (Ellaway et al., 2005; Tang & Long, 2019). Such approaches may involve physically transporting evaluators to real locations for direct evaluation of environmental attributes, which can be time-consuming, expensive, and subjective to each participant (Gupta et al., 2012; Meitner, 2004; Yao et al., 2012). In contrast to interview approaches, recent computational advances (e.g., Deep learning image analysis) along with high-

resolution data from multiple sources such as geospatial data and street view image data allowed computational modelling of eye-level greenery at scales.

One example is the geospatial viewshed model using high-resolution light detection and ranging (LiDAR) based data, which has been extensively employed to map and quantify vegetation cover in urban areas, benefiting from their advantages in terms of repeatability, synoptic view, and wide area coverage (Li, Zhang, Li, Ricard, et al., 2015). These methods involve three-dimensional data sets derived from high-resolution remotely sensed images and LiDAR, enabling the detection of tree species and the vertical dimensions of urban trees (Alonzo et al., 2014; Edson & Wing, 2011; Shrestha & Wynne, 2012). According to Yu et al. (2016), these approaches offer several advantages, such as the capacity to adjust the relative height of the observer to simulate different vertical horizons and the potential to model artificial buildings to simulate future landscapes. Nevertheless, the results depend on the original resolution and accuracy of the utilised datasets (Labib et al., 2021), and there is a risk of information loss when compressing point cloud data into a two-dimensional raster surface (Yang et al., 2020). Additionally, high-resolution LiDAR data and digital elevation raster surfaces are mostly unavailable in most cities or countries worldwide, making it difficult to use such models in diverse geographic contexts (Labib et al., 2020, 2021). Furthermore, this data may not fully capture the visibility and perception of street tree canopies from the viewpoint of pedestrians. The disparity between the profile view and overhead view becomes evident, for example, when comparing observations for urban forests and green walls (Li, Zhang, Li, Ricard, et al., 2015; Lu, 2019; Yang et al., 2009).

In contrast to the viewshed based approach, Li et al. (2015) made significant advances in this field by utilising automatically extracted Google Street View (GSV) images and employing image segmentation techniques for automating the greenery calculation process. This breakthrough has led to the emergence of several innovative computational approaches that have demonstrated a high level of agreement with human perception (Aikoh et al., 2023; Suppakittpaisarn et al., 2022; Torkko et al., 2023), offering several benefits such as reduced research time and workloads, increased accessibility, and the ability to study urban greenery without the need for physical visits to field sites (Lu et al., 2023; Rangel et al., 2022).

One widely adopted approach is computational image segmentation, which is categorised into colour-segmentation and semantic-segmentation. Colour-segmentation method classifies images according to colour values of individual pixels, effectively identifying and delineating areas with green vegetation (J. Chen et al., 2020; Dong et al., 2018; Larkin & Hystad, 2019; Long & Liu, 2017). On the other hand, semantic-segmentation is a machine learning-based approach that leverages contextual information to understand and segment images (Xia et al., 2021). By assigning semantic levels to individual pixels, this method allows to comprehend the image content, facilitating precise identification and mapping of green vegetation (Cai et al., 2018; Helbich et al., 2019; Ki & Lee, 2021; Kido et al., 2021; Xia et al., 2021; Ye et al., 2019). Recently, Torkko et al. (2023) investigated different eye-level greenery extraction methods and found that the image segmentation approach better aligns with human perception than colour-based segmentation. The colour-based segmentation approach is sensitive to lighting conditions, resulting in unquantified greenery when faced with dimly lit or brightly lit environments (Batlle et al., 2000; Pietikainen et al., 1996). Additionally, this approach tends to misclassify green paint as greenery, leading to overestimation of green areas (Larkin & Hystad, 2019; Li, Zhang, Li, Ricard, et al., 2015).

Numerous recent studies employing image segmentation for vegetation analysis heavily rely on data from GSV (Cai et al., 2018; S. Chen & Biljecki, 2023; Jimenez et al., 2022; Rzotkiewicz et al., 2018). However, it is crucial to acknowledge the barriers and limitations surrounding data access and usage (Inoue et al., 2022; Zheng & Amemiya, 2023). In particular, GSV imposes restriction on the use of imagery, including limitations on data analysis and extraction (Google, 2018b, 2020). As stated by Rundle et al. (2022), the restriction on certain uses of Google Maps is not grounded in copyright law, which would potentially allow researchers to invoke FAIR (Findable, Accessible, Interoperable and Reusable) use principles. Rather, these limitations are based on the contractual agreement that users must adhere to when accessing Google Maps (Google, 2018a). The enforceability of such contracts is currently subject to ongoing legal disputes, making it uncertain. Consequently, researchers engaging in this type of research and the journals publishing the resulting papers assume some legal risk as long as the legal status remains unsettled (Rundle et al., 2022; Stringam et al., 2023). In addition, using such data might hinder the adoption of FAIR data principles in scientific research (Wilkinson et al., 2016). GSV is often easy to find, and interoperable with other data (e.g., provided by Google). However, it is not

widely accessible due restrictions to number of free downloads, there is a limit to the quantity of data that can be obtained without incurring charges (Google, 2023; Zheng & Amemiya, 2023). Meaning, researchers who require a considerable amount of GSV data may encounter financial barriers to accessing them. This inaccessibility also results in lack of reusability of such data by others. As whole GSV data mostly does not meet the FAIR data principles.

To overcome GSV limitations, integrating Volunteered Street View Imagery (VSVI) platforms, such as Mapillary and Open Street Cam, has been developed over the years (Alvarez Leon & Quinn, 2019; X. Yu et al., 2019; Zheng & Amemiya, 2023). Mapillary, in particular, stands out as the largest crowdsourcing-based street view platform, boasting a community of over 20,000 users who contribute street-level photos using GPS-enabled cameras or smartphones (Ma et al., 2020). Notably, Mapillary adopts an open data approach by realising imagery under the Creative Commons Attribution-ShareAlike 4.0 International license (Alvarez Leon & Quinn, 2019). This open data policy enables researchers to utilise the imagery more freely, including for commercial purposes, fostering innovation and collaboration in studying urban greenery and related phenomena (Alvarez Leon & Quinn, 2019).

While Mapillary provides an alternative solution through its open data approach, researches are aware of its limitations, as these can affect the reliability and accuracy of the data (Antequera et al., 2020; D'Andrimont et al., 2018; Juhász & Hochmair, 2016; Krylov & Dahyot, 2019). Firstly, the quality of the imagery contributed by users on Mapillary may vary significantly due to differences in camera properties, including various camera models and settings used by contributors (Antequera et al., 2020). These variations can result in differences in resolution, blurring, restricted field of view, and reduced visibility (D'Andrimont et al., 2018). Secondly, Mapillary primarily relies on forward-facing cameras mounted on vehicles driven on roads, resulting in linear motion without rotation, limiting the perspectives captured in the imagery and potentially limiting the comprehensive understanding of the surrounding (Antequera et al., 2020; Krylov & Dahyot, 2019). Finally, the level of engagement and participation from users can vary across different regions and communities, leading to disparities in data availability (D'Andrimont et al., 2018; Nielsen, 2006). As a result, researchers relying solely on Mapillary may encounter gaps in the coverage of specific locations or road segments that can limit the ability to obtain a complete and representative sample of the desired study area (Juhász & Hochmair, 2016).

In contrast to missing street view image in certain locations, satellite-derived top-down measures of greenery, such as the Normalised Difference Vegetation Index (NDVI), is globally available at any place and often widely used in measuring greenness modelling (Martinez & Labib, 2023). It can be argued that for situations where there is insufficient street image data to determine the GVI, an alternative approach is to utilise the NDVI to estimate GVI using statistical models. Although NDVI is a top-down measure and may not fully capture the actual visibility of greenery (Labib et al., 2021), it represents available vegetation, thus it can be assumed that a model can learn from the relation between known GVI and NDVI within a certain distance zone to impute GVI for unknown locations. In this regard, Torkko et al. (2023) indicated that mean NDVI values within smaller distances (e.g. 50 m) from observation points might produce accurate representations of perceived visible greenery. In a different research, O'Regan et al. (2022) demonstrated a methodology to estimate air pollution, incorporating GVI, NDVI, and other variables. Thus, using NDVI to estimate GVI can be a potential solution to fill the street view data gaps for modelling greenness visibility.

A few studies have demonstrated the potential of utilising Mapillary's images for evaluating and quantifying urban greenness visibility (Liang et al., 2022; Yap et al., 2022), and numerous studies have used NDVI to measure the presence of greenery (Martinez & Labib, 2023). Despite these promising findings regarding the potential use of the data source, there remains an absence of systematic evaluation regarding the usability of Mapillary data in different urban contexts for estimating greenness visibility and the potential of using NDVI to estimate greenness visibility in missing locations. Additionally, there is a lack of complete methodological workflow to use Mapillary data in different places and reproduce these analyses, hindering the usage of such open-source and FAIR data in modelling greenness visibility in diverse geographic contexts.

To address the methodological limitations and existing research gaps noted above, this study aims to provide a scalable, reproducible methodological framework for utilising Mapillary data for greenness visibility modelling as well as evaluate the completeness and usefulness of such data in diverse geographical contexts. The primary objective is to establish a robust and replicable methodology that can be applied for greenness visibility modelling at any locations. Additionally, the secondary objective of this study is to evaluate the use of NDVI to estimate GVI in locations

where street view images are unavailable. To achieve these objectives, this study will examine the following research questions:

RQ1) How does the image availability and usability of Mapillary data for green view assessments change across different cities worldwide?

RQ2) To what extent is the Normalised Difference Vegetation Index (NDVI) suitable for filling in missing data points in the Green View Index (GVI) assessment?

RQ3) Are there differences in street level greenness visibility between cities located in different geographic contexts?

To answer these questions, we will conduct a comparative analysis of the GVI across different cities worldwide, allowing to assess the quality and completeness of the data available through Mapillary. This comparative approach will provide insights into the reliability and applicability of the platform for green view assessments in different parts of the world.

The development of this methodology aims to democratise the analysis of urban greenness, making it FAIR to researchers, urban planners, and policymakers interested in assessing and monitoring the visibility of green spaces in their cities. By establishing a methodology, our project seeks to fostering a better understanding of the relationship between urban environments and human well-being.

2. Methodology

2.1 Study area

Our study examines a diverse range of cities across diverse geographic, demographic, and socioeconomic contexts and located in multiple countries and continents. The cities included in our research are City of Melbourne, Australia; Amsterdam, Netherlands; Kampala, Uganda; Tel Aviv, Israel; Seattle, USA; Mexico City, Mexico; and Dhaka, Bangladesh. City of Melbourne, Amsterdam, Seattle, and Tel Aviv are known for their advanced urban planning and commitment

to environmental sustainability initiatives (Bush et al., 2021; Dierwechter, 2017; Herscovici et al., 2022; Mora & Bolici, 2017). These cities, situated in developed nations, have been able to invest significantly in their infrastructure, incorporating technology and innovation to enhance their urban environments (Bush et al., 2021; Dierwechter, 2017; Herscovici et al., 2022; Mora & Bolici, 2017). In contrast, Kampala, Dhaka, and Mexico City, located in developing regions, face unique challenges related to rapid urbanization (Abebe, 2013; Aguilar & Lopez, 2018; Mortoja & Yigitcanlar, 2022). These cities experience high population growth and are often facing with issues of limited resources, both in terms of infrastructure and public services (Abebe, 2013; Aguilar & Lopez, 2018; Mortoja & Yigitcanlar, 2022). Their inclusion in the study provides a contrasting perspective on urban development and the role of Volunteered Street View Imagery (VSVI), such as Mapillary, in such dynamic and resource-constrained contexts. Since one of our aims is to evaluate the quality and completeness of the data available through Mapillary, we assume that these diverse cities will provide valuable insights into the reliability and applicability of the platform for assessing green views in different parts of the world. It will also allow to identifying variations or limitations in the data that may exist between cities.

2.2 Data Sources

The data sources for this study primarily consisted of open-source platforms, which provided access to a wide range of geospatial data. Three major data sets were utilised in this research, namely: the Street Network with OSMnx, the VSVI with Mapillary, and the Satellite-Derived NDVI.

2.2.1 Street Network with OSMnx

Street network data was retrieved using OSMnx, an open-source Python library specifically developed for working with Open Street Map (Boeing, 2017). OSMnx provides a convenient set of functions and methods for downloading and processing street network graphs for specific regions (Boeing, 2017). Our research employed this library to extract simplified street network data, with a specific focus on obtaining edges information.

2.2.2 VSVI with Mapillary

The VSVI data was obtained by using the Mapillary API (Mapillary, 2021). The API provides access to vector tiles endpoints that contains information such as the position of images and sequences with their original geometries. Within the coverage tiles endpoint, three layers are available: overview, sequence, and image. For our research, we focused on the image layer, which contains details such as the compass angle of the image, the timestamp of image capture, the image ID, and a flag indicating whether it is a panoramic image.

2.2.3 Satellite-Derived Normalised Difference Vegetation Index

The Satellite-Derived NDVI data were used in our study to determine the GVI on points in areas where images were unavailable. Specifically, the NDVI data was derived from Sentinel-2 satellite imagery, which offers a resolution of 10 metres (Satellite Imaging Corporation, 2022). To ensure the quality and reliability of the NDVI data, certain criteria were applied to selecting satellite imagery. Firstly, the chosen imagery had a cloud cover of less than 10% to mitigate the potential distortion caused by clouds, which can obstruct the accurate assessment of vegetation indices (Meraner et al., 2020). Secondly, the selected satellite imagery was collected considering the best pixel over the course of the year 2020. This approach involved selecting the image with the most favourable conditions for vegetation analysis within the given time frame, maximising the accuracy and representativeness of the NDVI data for the analysis (Corbane et al., 2020). We used estimate NDVI Google Earth Engine (GEE) to identify images within the period spanning the first and last day of 2020, from which a composite image was generated. The composite image consisted of pixels with the median value across all identified pixels based on the criteria noted above. The NDVI values range from -1 to +1, where a value of -1 represents water, values around 0.2 suggest vegetation coverage, and higher values indicate denser forest coverage. To ensure that only image pixels potentially containing vegetation were considered, values below 0 were removed from the analysis.

2.3 Modelling GVI using open source data

Step 1. Retrieve Street Road Network and Generate Sample Points

Figure 1 shows an overview of our methodology. First, the simplified street network data, represented as a graph object with nodes and edges, was obtained from OSMnx by indicating the name of the city to be analysed (e.g., "Amsterdam, Netherlands"). It is worth noting that bidirectional streets are represented as two separate overlapping roads, with the starting and ending nodes inverted. To avoid analysing the same road twice, we implemented a filtering strategy to retain only one of the duplicate roads.

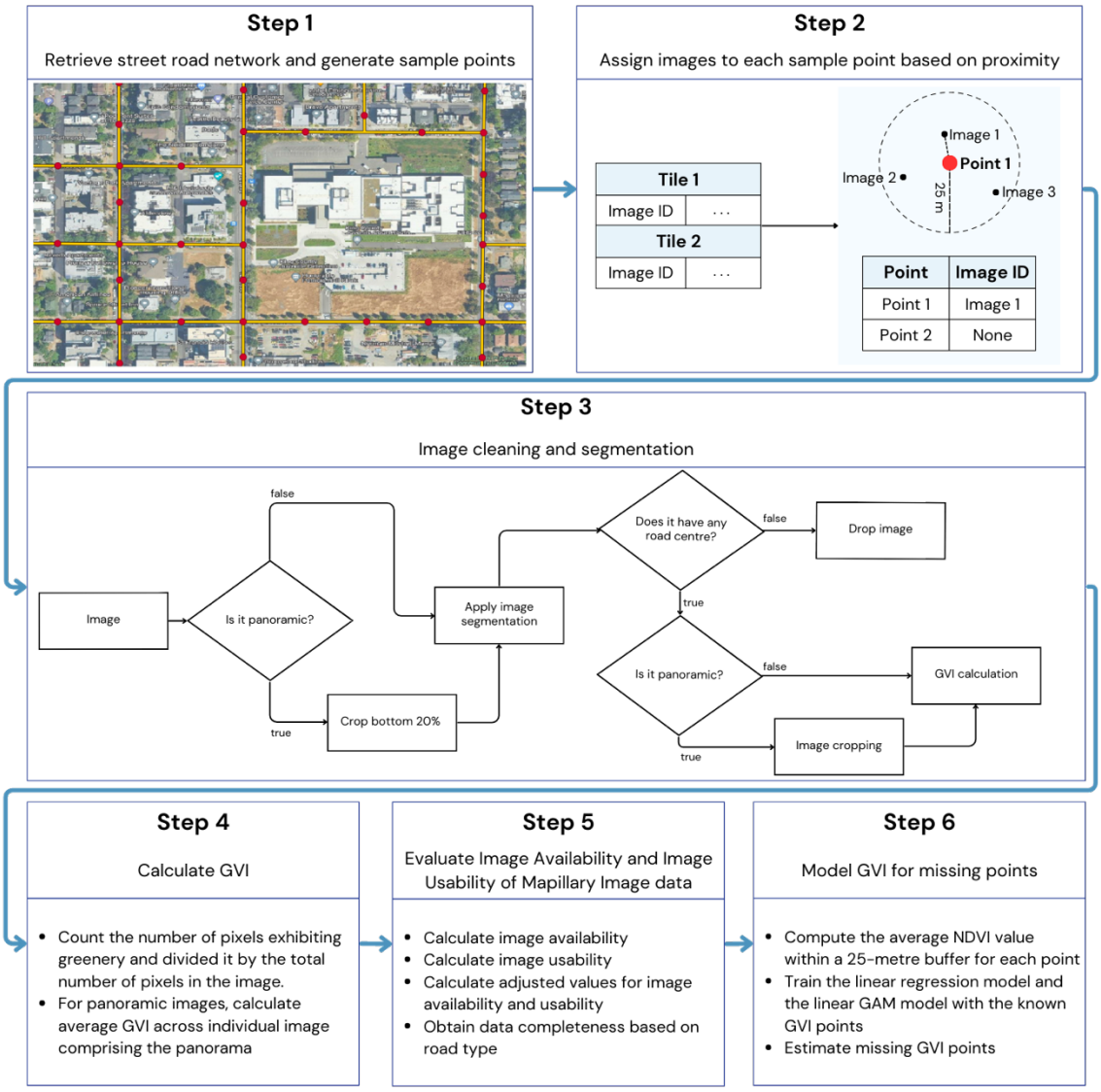

Figure 1: Methodology overview, which is openly accessible in GitHub.

Once the street network data was projected, we proceeded to conduct point sampling at regular intervals of 50 metres along the roads. These sampled points serve as reference locations for selecting the corresponding images from Mapillary, which were then used to analyse the GVI.

Step 2. Assign Images to Each Sample Point Based on Proximity

To access the VSVI data, requests need to be made to the Mapillary API using the tile coordinates and zoom level of 14 (Mapbox, 2023). Therefore, to implement the data retrieval, we divided the area covered by the obtained road network into tiles. For each tile, we accessed the metadata of all the available images within it. Subsequently, we assigned one image to each sample point in the road network based on their proximity using the cKDTree algorithm provided by the SciPy library (SciPy, 2022). This algorithm constructs a k-dimensional tree structure that facilitates efficient querying of nearest neighbours. In our case, the tree was queried to identify the closest neighbour within a maximum distance of 25 metres from each sample point. This distance was chosen based on the spacing of the sample points, which are 50 meters apart. By using this distance, we can ensure that no two points will be assigned the same image.

Once we had determined the image ID of the closest image to each sample point, we were able to access the corresponding image by using the URL provided by the image endpoint (Mapillary, 2021). Specifically, we accessed the URL to the original wide thumbnail of the image, which provided us with a visual representation of the image that could be further analysed to obtain the GVI on the sample point.

Step 3. Image cleaning and segmentation

After obtaining the image, the subsequent step involved semantic image segmentation and image filtering process to clean and segment the images for further processing. To begin, for panoramic images, we performed a cropping operation to remove the bottom 20% of the image. This area corresponds to a band captured by the camera that is present in all panoramic images. By removing this band, we ensured that only the relevant portions of the image were retained for further analysis.

In the next stage, we applied the Masked-attention Mask Transformer (Mask2Former) architecture based image segmentation model (Cheng et al., 2022) to segment the images in

different objects. The Mask2Former (Figure 2) is a powerful architecture designed for universal image segmentation, encompassing tasks such as panoptic segmentation, instance segmentation, and semantic segmentation (Cheng et al., 2022). To achieve its capabilities, the Mask2Former model incorporates several key components. One of the central elements is the use of masked attention, a mechanism that enables the extraction of localised features by constraining cross-attention within predicted mask regions. By doing so, the model can focus on relevant regions and capture fine-grained details, resulting in highly accurate segmentation results (Cheng et al., 2022).

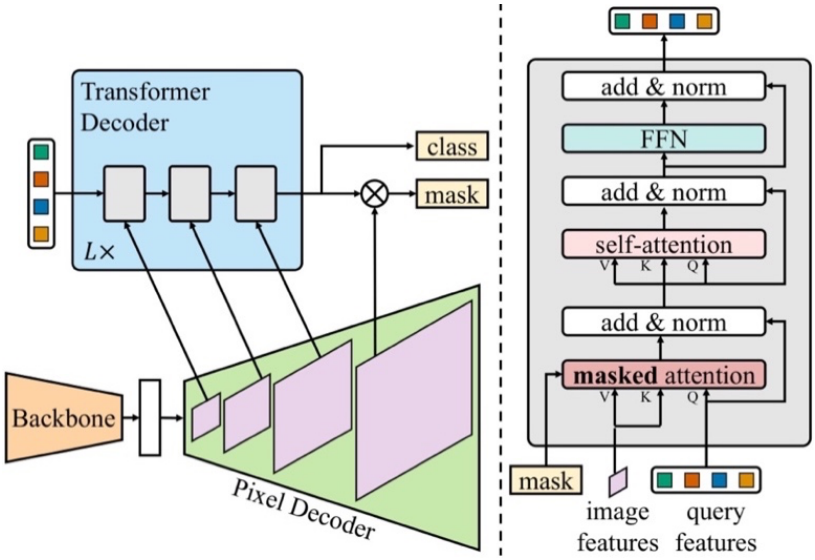

Figure 2: Mask2Former architecture (Cheng et al., 2022)

The performance of Mask2Former was evaluated on four popular datasets: Common Objects in Context (COCO), Cityscapes, ADE20K, and Mapillary Vistas (Cheng et al., 2022). Notably, when tested on the Mapillary Vistas dataset, the model achieved impressive mean intersection over union (mIoU) scores of 57.4 for small objects and 59.0 for medium and large objects. These results underscore the competitive performance of Mask2Former compared to other state of-the-art methods on Mapillary Vistas (Cheng et al., 2022). In our study, Mask2Former enabled the identification and classification of different objects within the images, including vegetation and roads, that were used for subsequent analysis.

To determine the suitability of each image for analysis, we employed an algorithm designed to identify road centres from the segmented image. If road centres were detected, then the image was considered suitable and retained for further calculation (Figure 3 a, b). Conversely,

if no road centres were identified, the image was deemed unsuitable and subsequently discarded (Figure 3 c, d).

This technique was applied to ensure we extract most representative viewing angle from the images, as many Mapillary images often has poor orientation and irregular camera angle (Figure 3 c, d). Therefore, excluding such images may improve the overall data quality and visibility estimation because irrelevant or less informative objects were removed. In cases where an image was both suitable and panoramic, we performed an additional cropping operation (Figure 3 a1, a2). The image was divided into "N" parts based on the identified road centres. This division allowed for a more focused examination of specific sections of the panoramic image and provide a holistic representation of the surrounding area.

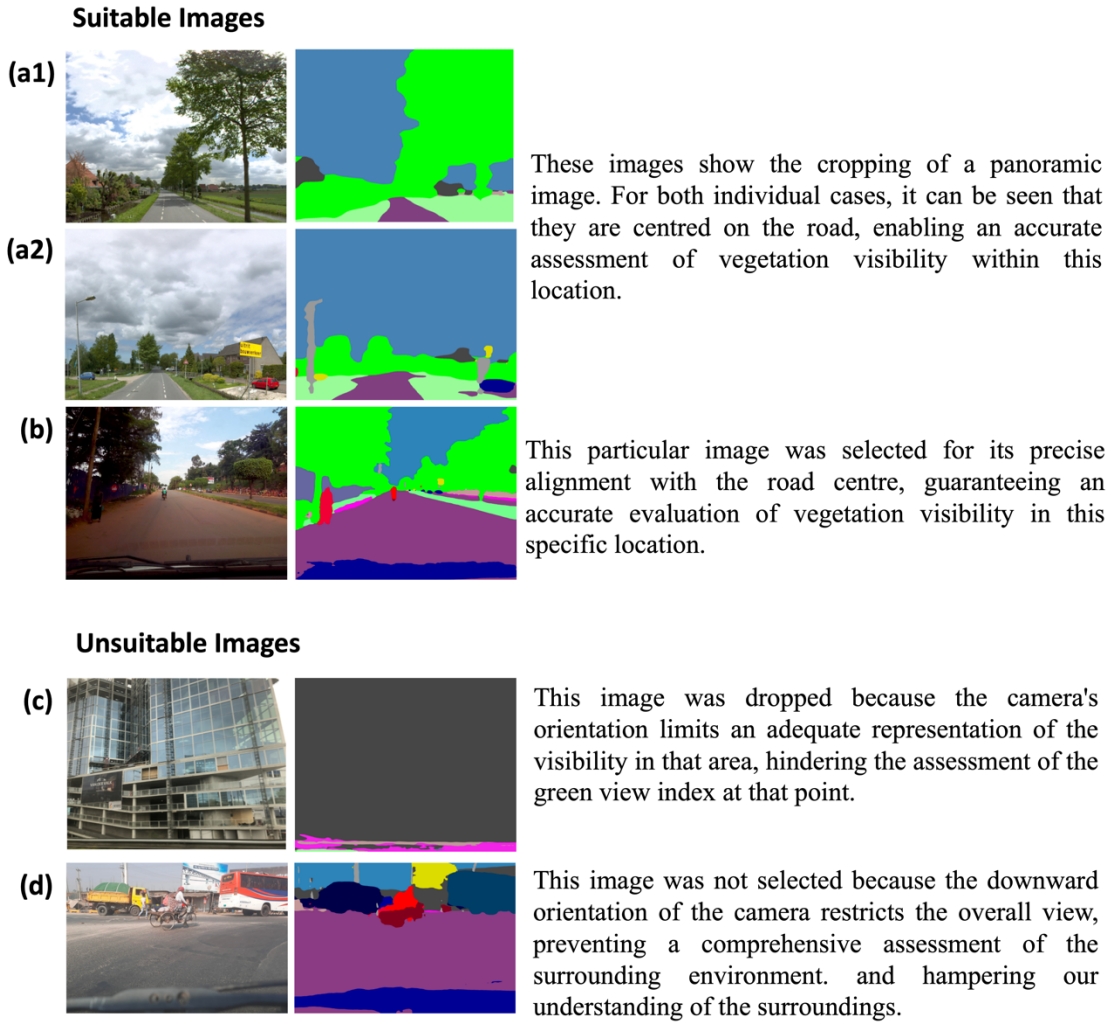

Figure 3: Examples of image segmentations and filtering criteria.

Step 4. Calculate GVI

The GVI equation used in this study was based on equation 1 proposed by Yang et al. (2009) for evaluating the visibility of urban forests. Their GVI calculates the ratio of the total green area from four pictures taken at a street intersection to the total area of the four pictures.

$$GVI = \frac{\sum_{i=1}^{4} Area_{green\_pixels\_i}}{\sum_{i=1}^{4} Area_{total\_pixels\_i}} \cdots (eq\ 1)$$

Where $Area_{green\_pixels\_i}$ represents the count of green pixels in the image captured in the *i*th direction (north, east, south, or west) at a specific intersection and $Area_{total\_pixels\_i}$ corresponds to the total number of pixels in the image captured in the *i*th direction. However, due to the unavailability of images captured in all four directions for all sample points in our dataset, we made a slight modification to the formula. The modified GVI we used can be expressed with equation 2.

$$GVI = \frac{\sum_{i=1}^{N} \frac{Area_{green\_pixels\_i}}{Area_{total\_pixels\_i}}}{N} \cdots (eq\ 2)$$

Where $Area_{green\_pixels\_i}$ is the number of green pixels in the *i*th picture found in the sample point, $Area_{total\_pixels\_i}$ is the total pixel number of the *i*th picture found in the sample point and N is the number of analysed pictures in the sample point. For non-panoramic images, N is equal to 1 since there is only one image available at the sample point. However, for panoramic images, N corresponds to the number of road centres identified at the sample point, indicating the number of cropped images.

Step 5. Evaluate Image Availability and Image Usability of Mapillary Image Data

In assessing image availability, we examined the presence of an assigned image for each sample point. Any sample point that did not have a corresponding image found within a 25-metre buffer was excluded. The availability of images in the dataset is expressed in equation 3 as the ratio of the number of sample points with assigned images ($N_{img\_assigned}$) to the total number of sample points N_{total}.

$$\text{Image Availability Score (IAS)} = \frac{N_{img\_assigned}}{N_{total}} \cdots (\text{eq } 3)$$

Similarly, in evaluating image usability, we focused on points that had assigned images and a known GVI value. This indicated that the image met the expected criteria for inclusion in the analysis. The quality of the data is represented in equation 4 as the ratio of the number of sample points with assigned images and known GVI values ($N_{img\_assigned \wedge GVI\_known}$) to the total number of sample points with assigned images ($N_{img\_assigned}$).

$$\text{Image Usability Score (IUS)} = \frac{N_{img\_assigned \wedge GVI\_known}}{N_{img\_assigned}} \cdots (\text{eq } 4)$$

Then, to enable a more meaningful comparison between cities of varying sizes, an adjustment was made to both scores by incorporating the natural logarithm of the road length in kilometres, as shown in equations 5 and 6. By applying this logarithmic transformation, the adjustment places greater emphasis on the relative differences in road lengths between cities, rather than absolute values.

$$\text{Adjusted Image Availability Score (AIAS)} = \frac{N_{img\_assigned}}{N_{total}} \times \ln(road\_length) \cdots \text{(eq 5)}$$

$$\text{Adjusted Image Usability Score (AIUS)} = \frac{N_{img\_assigned \wedge GVI\_known}}{N_{img\_assigned}} \times \ln(road\_length) \cdots \text{(eq 6)}$$

In addition to the availability and usability assessment, we conducted further analysis to provide additional insights. Firstly, we measured the proportion of panoramic images in each city. This assessment allows us to evaluate the availability and coverage of panoramic imagery, which can provide a more comprehensive view of the city's surroundings. Furthermore, we examined the types of roads (e.g., residential, primary, secondary roads) with the most missing images. By identifying the specific road types where the image coverage is limited, we can gain insights into potential gaps in the dataset. This information is valuable for understanding the limitations and areas that require further attention in improving the availability of images for analysis.

Step 6. Model GVI for missing points

To estimate the GVI values for the missing data points, we employed two modelling approaches per city: Linear Regression and Linear Generalised Additive Models (GAM). In both cases, we utilised the NDVI raster file of each city. For each point in the dataset, we computed the average NDVI value within a fixed-size buffer surrounding the point. After conducting tests with multiple buffers of 100, 50, and 25 metres, it was determined that the buffer of 25 metres exhibited the best model performance. Subsequently, we employed the points with known GVI values and their corresponding calculated NDVI values to train both the Linear Regression and the Linear GAM models. The performance of these models was evaluated using the Root Mean Square Error (RMSE) through cross-validation with 5 folds. Additionally, to facilitate a comparison between the two models, we computed the Akaike Information Criterion (AIC) score. Finally, both models allowed us to estimate GVI values based on the available GVI and NDVI data in each city, thereby completing the information for the missing points.

2.6 Computational resources

The data processing and analysis for this study were implemented using the Python programming language. Python provides a wide range of libraries and tools that facilitated the handing and manipulation of de data, as well as the implementation of various algorithms and models.

To execute the code, we utilised Google Colab, a cloud-based platform that offers a Python development environment along with access to powerful hardware resources. The Google Colab environment provided several advantages, including the availability of a high amount of RAM and GPU acceleration, which significantly contributed to the efficiency of the image segmentation process. For this research, we employed a computational system with 25.5 GB of RAM and a T4 GPU accelerator with a 15 GB memory capacity.

This configuration allowed us to handle large datasets and smoothly execute memory-intensive operations, resulting in a substantial reduction in processing time for each image. Additionally, we implemented parallel processing techniques to enhance the efficiency of the image segmentation process and maximise the utilisation of the available computational resources. Through the combination of these implemented techniques and computational resources described above, we achieved high processing capabilities that enabled us to analyse approximately 4,000 images within a span of 40 minutes.

3. Results

3.1 Image Availability and Image Usability of Mapillary Image Data

After designing and implementing the methodology to calculate the GVI using Mapillary data in any city worldwide, we obtained the GVI information for seven different cities. In order to provide a comprehensive overview of our findings, we will first address Research Question 1, which involves comparing the GVI across different cities and evaluating the availability and usability of image data obtained through Mapillary. Figure 4 provides a visual representation of

the calculated GVI values using exclusively Mapillary image data, highlighting disparities in image availability across the selected cities. Figure 4a corresponding to Seattle, Figure 4b to Amsterdam, and Figure 4g to City of Melbourne, consistently exhibit the highest degree of image availability. This observation aligns with the high AIAS achieved by these cities, as shown in Table 1. On the other hand, our findings reveal a contrasting picture for Figure 4c corresponding to Tel Aviv, Figure 4e to Dhaka, and Figure 4f to Kampala, which also exhibit significantly lower AIAS. Intriguingly, Figure 4d shows a significant disparity in image availability within Mexico City, with its southern region displaying considerably fewer images compared to the central area.

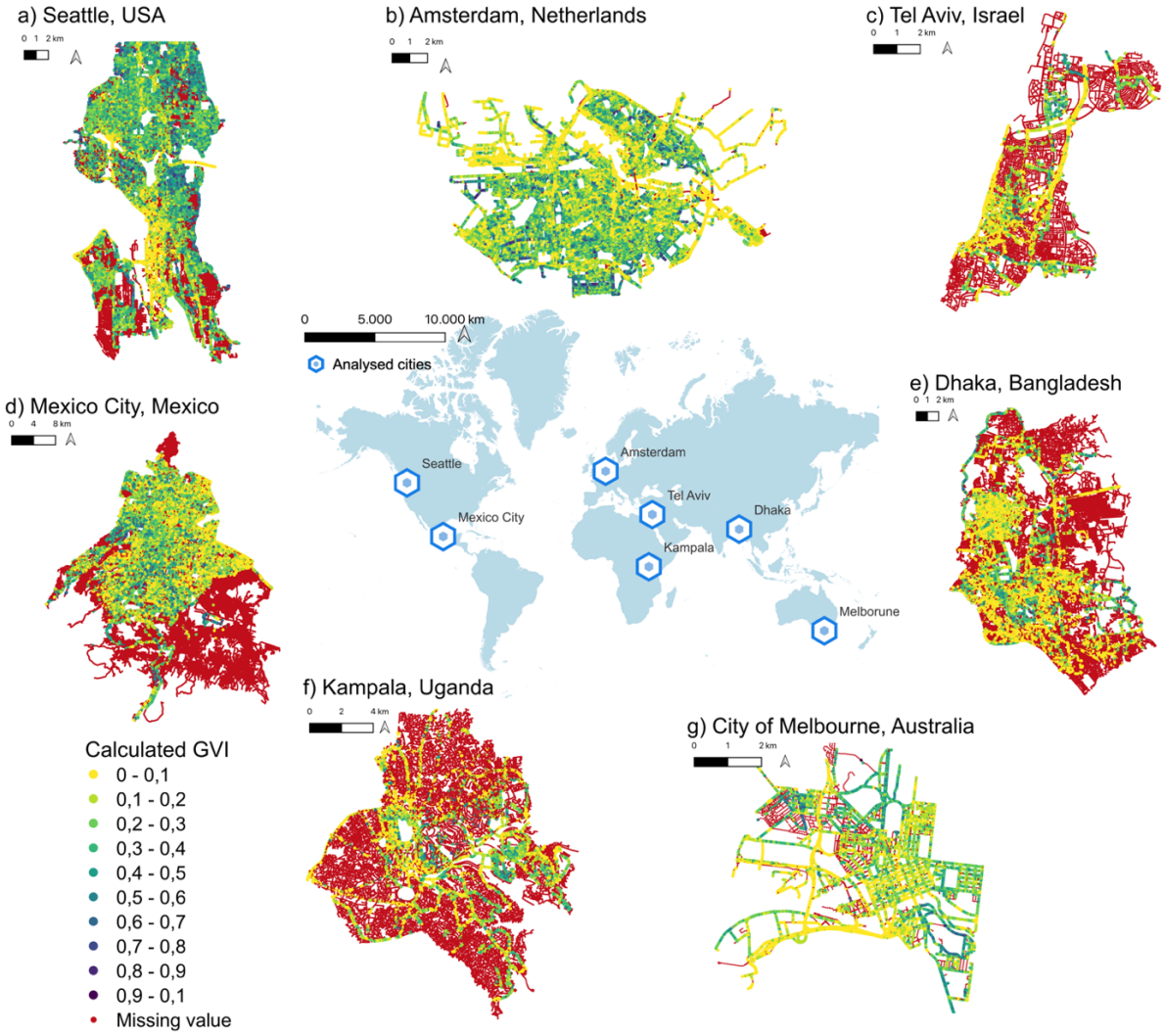

Figure 4: Calculated GVI across different cities using Mapillary Image Data.

Regarding the usability, as presented in Table 1, our findings provide intriguing insights into the usability of street-view imagery, adjusted for city size, in our seven cities of interest.

Notably, Mexico City stands out with the highest AIUS, suggesting that despite the uneven distribution of image availability as indicated in Table 1, the proportion of usable images remains high. Similarly, Tel Aviv, exhibits a relatively high IUS despite having the lowest availability in Table 1, indicating that although the volume of images in this city was lower, the proportion of usable images was high. Furthermore, Amsterdam once again demonstrates a high AIUS, consistent with its high Image Usability Score. This consistency indicates that the robustness of the usable image data in this city is largely maintained, even after accounting for city size.

City	IAS	AIAS	IUS	AIUS
Tel Aviv	0.3739	3.0118	0.7829	6.3064
Kampala	0.3461	3.1067	0.5499	4.9362
Dhaka	0.3764	3.6895	0.8355	8.1887
Mexico City	0.4468	4.9863	0.8469	9.4514
City of Melbourne	0.8371	6.4510	0.8906	6.8629
Seattle,	0.7610	7.2340	0.8271	7.8632
Amsterdam	0.9871	9.2057	0.9570	8.9252

Table 1: Image Availability Score, Adjusted Image Availability Score, Image Usability Score and Adjusted Image Usability Score for each analysed city

In terms of panoramic images, the data presented in Table 2 reveals a considerable difference in the availability of panoramic images. Amsterdam stands out prominently with the highest number, as more than 80% of its images are panoramic. In contrast, the remaining cities exhibit considerably lower proportions of panoramic images. For instance, Dhaka did not have any panoramic images in its dataset, while Mexico, City, City of Melbourne, Kampala and Tel Aviv all have less than 2% of their total images classified as panoramic.

City	Panoramic Images	Total Images	Proportion
Dhaka	0	31078	0
Mexico City	689	137994	0.0049
City of Melbourne	52	8693	0.0059
Kampala	197	14162	0.0139
Tel Aviv	128	6325	0.0202
Seattle	7069	47031	0.1503
Amsterdam	32216	38040	0.8468

Table 2: Proportion of Panoramic Images for each analysed city.

Next, we analysed the presence of missing values in each street of the cities, identifying the top five highway types with the highest number of missing images. Furthermore, we calculated the proportion of missing images corresponding to each category in every city. Our analysis revealed a consistent trend across all cities, with residential streets displaying the highest proportion of missing images, as depicted in Figure 5. Figure 5 illustrates that not only do residential streets have the highest volume of missing images in each city, but this deficit is notably significant, with all cities surpassing a 30% mark. This consistent and substantial percentage underscores a significant data gap within residential areas.

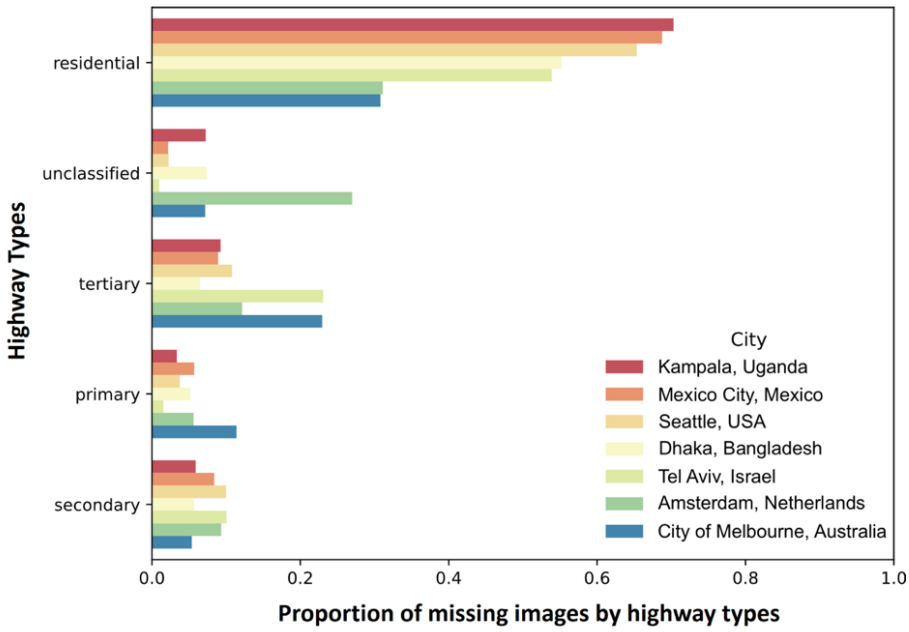

Figure 5: Top 5 Highway Types with Most Missing Images.

3.2 Modelled GVI for missing points using NDVI

Regarding Research Question 2, the viability of using NDVI to fill in missing data points was assessed by utilising Linear Regression and Linear GAM. Our results, shown in Table 3, reveal some key insights. Across cities, Linear Regression consistently resulted in lower RMSE values compared to Linear GAM, indicating a more accurate model with smaller residuals. The AIC scores highlight a consistent preference towards the Linear Regression models over the Linear GAM models across all cities. For instance, in Seattle, the Linear Regression model resulted in an AIC of -161384.4018, while the Linear GAM model yielded a less effective AIC of -136175.2627. This pattern is repeated across all examined cities, indicating a more favourable balance of fit and simplicity for the Linear Regression models when predicting GVI with NDVI.

City	Linear Regression		Linear GAM	
	RMSE	AIC	RMSE	AIC
Tel Aviv	0.1271	-20422.5508	0.1458	-19060.8670
Kampala	0.1222	-32733.2024	0.1449	-30080.0228
Dhaka	0.1242	-108314.5968	0.1434	-100829.2755
Mexico City	0.1239	-488017.0528	0.1621	-425206.4704
City of Melbourne	0.1305	-31516.7640	0.1505	-29316.2603
Seattle	0.1256	-161384.4018	0.1737	-136175.2627
Amsterdam	0.1660	-130717.0516	0.1832	-123572.8984

Table 3: RMSE and AIC values for Linear Regression and Linear GAM model across all analysed cities.

Furthermore, Figure 6 shows the trend line and R-squared values observed across the tested cities, showing a relatively low value for most of them. However, the comparatively lower RMSE values obtained in our study indicate that, despite the low R-squared values suggest a degree of unexplained variability, the RMSE values provide a more optimistic outlook on the utility of our models for predicting GVI using NDVI.

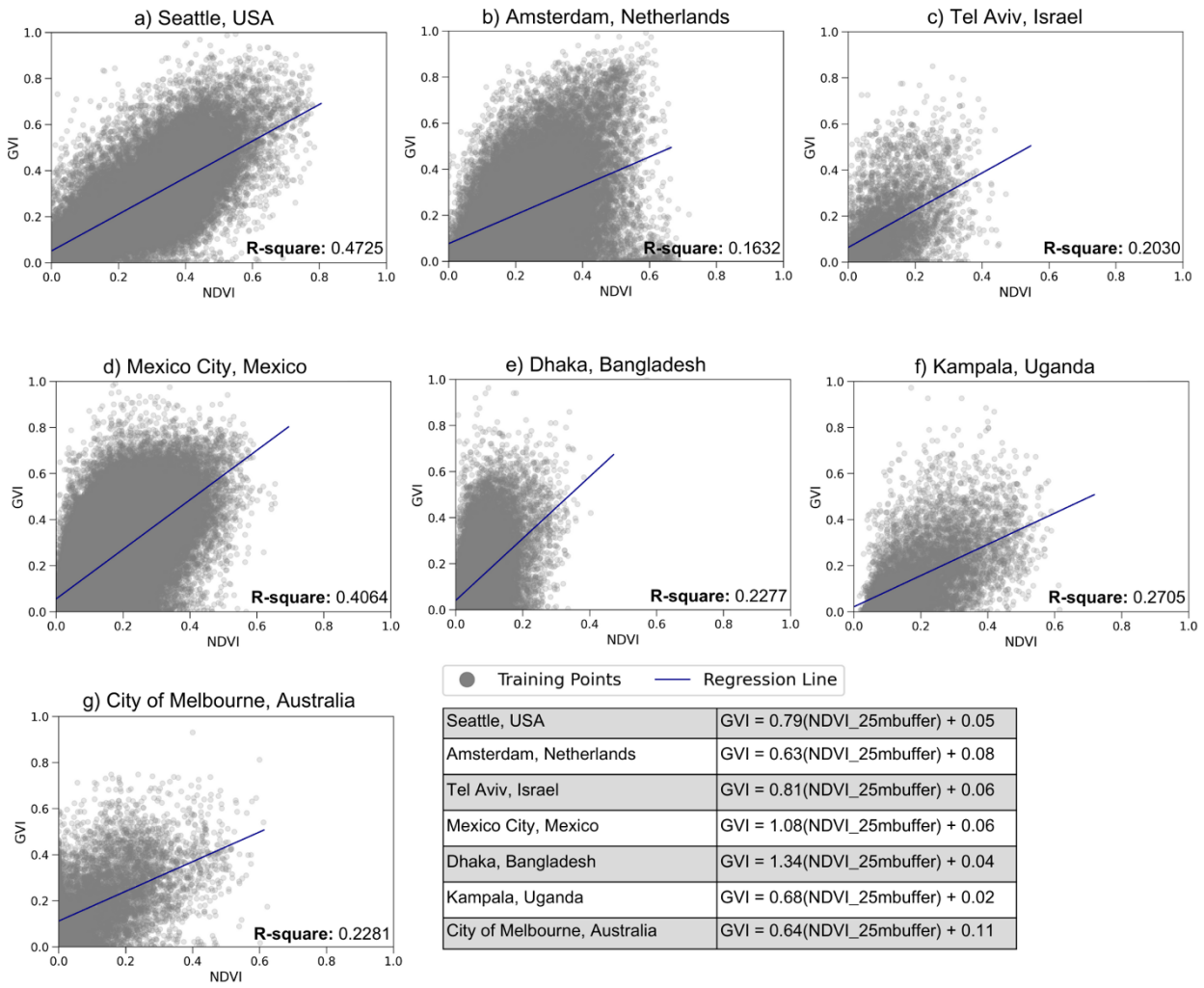

Seattle, USA	GVI = 0.79(NDVI_25mbuffer) + 0.05
Amsterdam, Netherlands	GVI = 0.63(NDVI_25mbuffer) + 0.08
Tel Aviv, Israel	GVI = 0.81(NDVI_25mbuffer) + 0.06
Mexico City, Mexico	GVI = 1.08(NDVI_25mbuffer) + 0.06
Dhaka, Bangladesh	GVI = 1.34(NDVI_25mbuffer) + 0.04
Kampala, Uganda	GVI = 0.68(NDVI_25mbuffer) + 0.02
City of Melbourne, Australia	GVI = 0.64(NDVI_25mbuffer) + 0.11

Figure 6: Linear regression trend lines and equations for each city.

Figure 7 provides a visual comparison between missing GVI values and their predictions using Linear Regression models for two contrasting cities: Amsterdam and Kampala. The black squares in the zoomed images show that the predicted GVI values closely align the calculated GVI values using street-view imagery for the surrounding points in both cities.

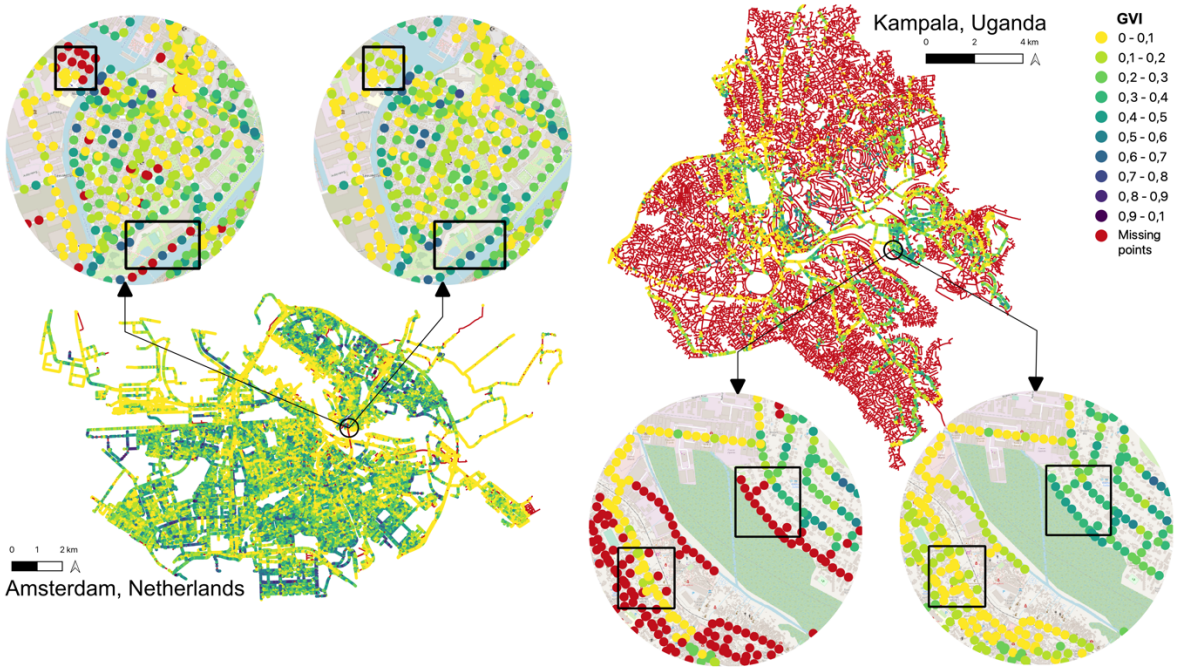

Figure 7: Comparing Image Availability between Amsterdam and Kampala, with GVI Estimation for missing points using a Linear Regression model for each city.

3.3 Mean and Median GVI comparison between cities

For Research Question 3, Figure 8 provides a visualisation of the mean and median GVI value for each street in the studied cities indicating the differences in street-level greenness visibility between cities. The GVI values show clear variations between developed and developing cities across continents in terms of green visibility. Seattle in North America has the higher value of 30.05% (Figure 8a), indicating abundant visible green spaces. In Europe, Amsterdam follows closely with a GVI of 22.38% (Figure 8b). However, Asian and African cities like Dhaka and Kampala have lower GVI values of 16.62% (Figure 8e) and 18.52% (Figure 8f), respectively. These variations underscore the disparities in green view visibility between developed and developing cities, with the former having a better supply.

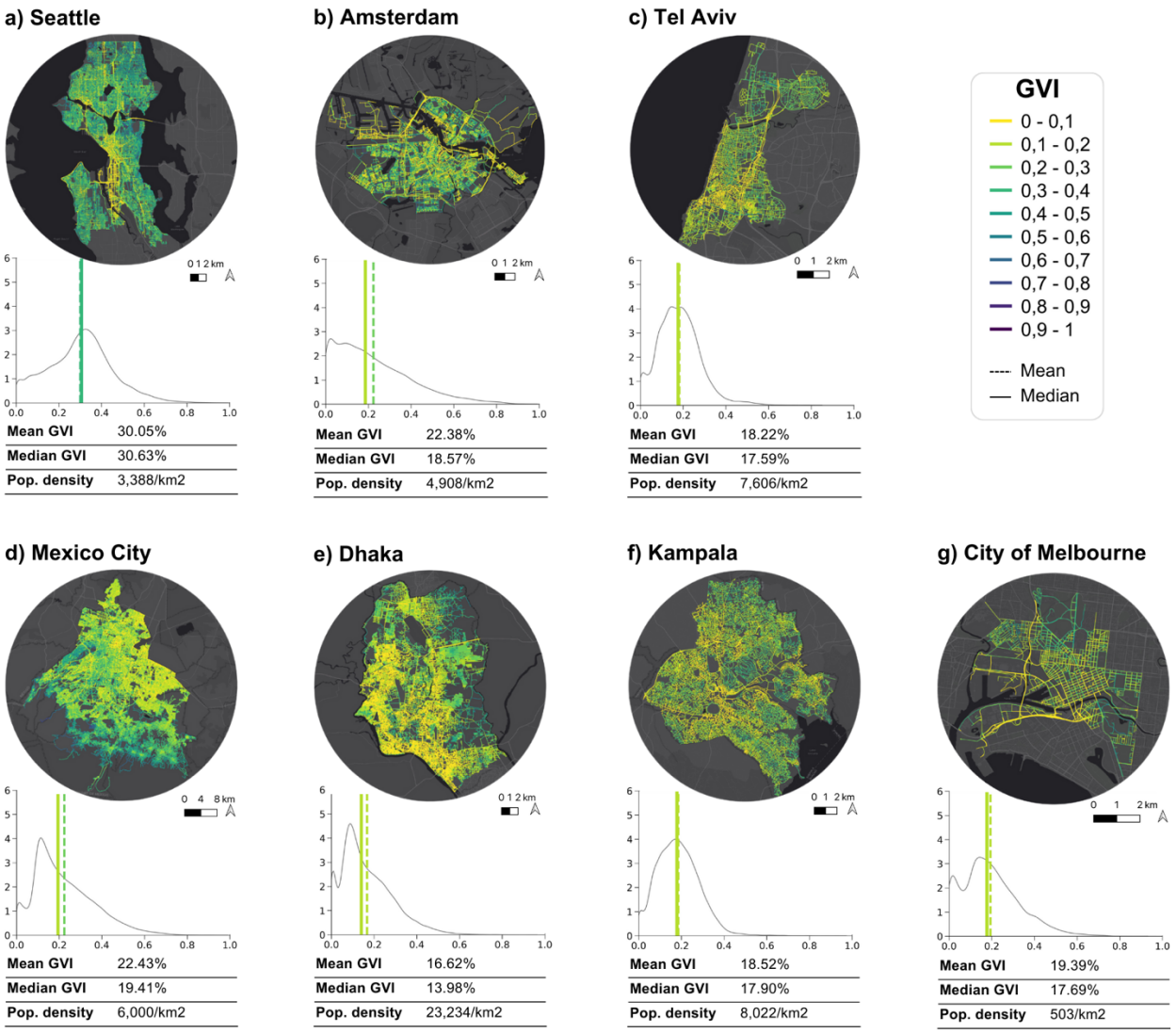

Figure 8: Mean and Median GVI per city along with their Density Plot, showing the different levels of street-level greenness visibility in diverse geographical contexts.

4. Discussion

4.1 Main findings

In this study, we aimed to develop a methodological framework for utilising open-source image data for greenness visibility modelling and evaluate the completeness and usefulness of such data in multiple cities in different countries worldwide. To our best knowledge, no previous

studies have developed such a methodology using open-source images (e.g., Mapillary) and implemented similar approaches in diverse geographic contexts. Our study revealed significant insights into using Mapillary data to calculate GVI across different cities worldwide, effectively addressing our first research question. We found that image availability, represented by the AIAS, varied significantly among the selected cities. Seattle, Amsterdam, and City of Melbourne consistently had high image availability, while cities like Tel Aviv, Dhaka and Kampala had much lower scores, as indicated in Figure 4 and Table 1. Interestingly, we found that the usability of images did not necessarily correlate with their volume. Table 1 shows that despite having fewer images, Mexico City and Tel Aviv had high AIUS indicating that a large proportion of the available images were usable. This suggests that meaningful GVI assessments are possible for places with usable images even though the city's overall image availability is limited. The distribution of panoramic images also showed a dramatic contrast across cities (Table 2). The disparity could impact the depth and breadth of GVI analysis, as panoramic images typically provide more comprehensive view of greenery in the surrounding area than a simple image with a limited view angle. Furthermore, our study pinpointed a considerable data gap in residential areas. We observed that these areas consistently showed the highest volume of missing images, as illustrated in Figure 5. This consistent deficit could pose potential challenges for comprehensive GVI assessments, highlighting the need for effective data supplementation methods. Our results are consistent with the previous study by Juhász and Hochmair (2016), who also demonstrated the availability of images varies considerable between countries and street types.

Addressing our second research question, our analysis also suggests that the NDVI can be used to calibrate a Linear Regression model for each city to fill in missing GVI data points with reasonable errors. In Figure 7 we illustrated that even in cities like Kampala, where the number of missing images is significantly high, estimated GVI values from NDVI align closely with those derived from street-view images. We argue that even though NDVI does not directly indicate the visibility of greenery, as they indicate the presence of vegetation, the modelled relations can reasonably estimate potential GVI values. Torkko et al. (2023) also observed that NDVI values might correspond to perceived visibility greenery.

To further validate the reliability of these findings, we compared our overall street-level GVI with data from MIT's Treepedia project (2023) conducted by the Senseable City Lab (Cai et

al., 2018). This comparison is relevant for several reasons. Firstly, Treepedia has a robust methodology, establishing it as an ideal reference point for our study (Cai et al., 2018; Li, Zhang, Li, Ricard, et al., 2015; Seiferling et al., 2017). Secondly, the similarity in our methodologies, specifically the application of semantic segmentation to assess street-view panoramas, fosters a direct and meaningful comparison. The key difference lies in our data sources, while Treepedia predominantly uses GSV, our study utilises Mapillary data.

Our analysis revealed that the median street-level GVI values for Amsterdam and Tel Aviv were similar to the estimates provided by Treepedia. However, in the case of Seattle, our approach slightly overestimated the overall GVI score. This discrepancy can be attributed to the limited availability of panoramic images in the Mapillary dataset (only 15% coverage in Seattle) compared to the predominantly panoramic GSV data used by Treepedia. Additionally, our study employed Normalised Difference Vegetation Index (NDVI) to estimate GVI in areas where data was missing, which was not implemented in the Treepedia project (Cai et al., 2018).

Finally, for the third research question, our analysis underscores a notable disparity in GVI across cities, particularly in high-density cities in Africa and South Asia. As Figure 8 illustrates, these densely populated, lower-income cities exhibit considerably less green visibility than low-density, high-income cities located in the USA and Europe. This is slightly suggested by the Treepedia data, but to our knowledge, no prior research has directly addressed this distinction. Moreover, the Treepedia project do not cover all geographical regions equally. For instance, their results do not include any cities in South Asia. Thus, our study is not only providing a reliable alternative method for GVI calculation but also extending the analysis to previously overlooked areas.

This disparity may be attributed to various factors, including the differences in urban planning strategies and investment in public spaces, the socio-economic development level, as well as the historical and cultural values assigned to green spaces in these regions. (Abebe, 2013; Dierwechter, 2017; Mora & Bolici, 2017; Mortoja & Yigitcanlar, 2022).

4.2 Strengths and limitations

Our study exhibits multiple strengths that reinforce its relevance within the urban green visibility research. Firstly, it used open-source, free, and FAIR data from Mapillary, making a significant stride in democratising and promoting open science in GVI assessments. This method establishes a standard for subsequent research while highlighting the effectiveness of open data for scientific purposes. Secondly, the scalability of the designed methodology in our research is a noteworthy aspect. Our approach to calculating GVI is not confined to the selected global cities but can be replicated and scaled for any city worldwide. This scalability is particularly significant considering the growing need for GVI assessments in urban spaces. Thirdly, our innovative approach in modelling visibility by combining GVI and NDVI represents a step forward in the field. By using NDVI and known GVI points we developed models that allows to fill in the missing GVI data points in a city, we provide a novel solution that holds the potential to expand and enhance the depth of GVI studies, even in contexts where street-view imagery data may be limited. Fourthly, it is important to emphasise that the code used in this study is reproducible. The implemented code is publicly available, thereby encouraging transparency, peer verification, and further innovation in the field. Reproducibility not only reinforces the validity of our findings but also empowers other researchers to build upon our work, advancing our collective understanding of urban green spaces and human well-being.

Nevertheless, our research had certain limitations that need to be acknowledge for a comprehensive understanding of our results. Despite the utility of Mapillary, we encountered poor image availability in Dhaka, Kampala, Mexico City, and Tel Aviv that can limit the assessment of GVI solely with street-view images. However, Amsterdam, City of Melbourne, and Seattle exhibited a more favourable situation regarding image availability. These disparities in image availability can be attributed to the socio-economic backgrounds of the cities (Fry et al., 2020) that may potentially lead to a less engaged community contributing to crowd-sourced database.

Another significant limitation was the temporal nature of our study, given that the Mapillary data were sourced at a specific point in time, and it may not be updated frequently or uniformly. The dynamic character of crowd-sourcing databases could mean that the image data might have been augmented, updated, or even rendered obsolete since our data collection.

However, these issues are not exclusively to Mapillary; even GSV imagery exhibits significant variability in availability and quality (Biljecki & Ito, 2021; Hara et al., 2013). Further, the infrequent updating of images impedes temporal assessment, as certain regions may remain unchanged for years (Hara et al., 2013). Such limitations are particularly evident in lower-income regions, rural areas, and countries in Africa, South America, and Southeast Asia, where GSV imagery remains unavailable or limited (Biljecki & Ito, 2021; Rzotkiewicz et al., 2018).

Moreover, a few specific limitations of using OSMnx for urban studies have been identified. One limitation is related to data availability and consistency, which is a recurrent issue in urban planning and street network analysis literature (Boeing, 2017). The data used by OSMnx, sourced from Open Street Map (Boeing, 2017), is provided by a community of contributors and thus, might not always be consistent or up-to-date. This means that any changes to the street networks that have occurred since the last update would not be reflected in the analysis. Furthermore, the reliance of OSMnx data quality and accuracy can vary considerably based on the location. The coverage of OSMnx is good across the United States and Europe, but developing countries might have less thorough street network coverage (Boeing, 2017).

Finally, while our study validated the use of NDVI to effectively fill in missing GVI data points, this approach is not devoid of challenges. NDVI primarily quantifies vegetation from bird's eye view and may not fully capture the nuances of human perception greenery (Labib et al., 2021; Larkin & Hystad, 2019), which is central to GVI. Thus, utilising NDVI to calculate missing GVI data points could introduce some inherent errors.

4.3 Future research

While this study has provided valuable insights into the usability of Mapillary data for calculating GVI, there are several promising avenues for further investigation. One potential area of investigation is obtaining a weighted average GVI value using population density in determined areas, which can provide a more accurate reflection of green visibility within a city. This approach can provide a more precise depiction of green visibility within a city, considering areas where the presence of greenery might be less perceptible due to low or negligible population density.

In addition to recognising the positive impact of green spaces on well-being, research has also highlighted the potential of blue spaces, such as bodies of water, in promoting human health. (Labib et al., 2020). Therefore, it would be valuable to explore the feasibility of integrating Mapillary data to calculate the Blue View Index for cities. This integration would enable researchers to investigate the influence of both green and blue spaces on various health indicators, providing a more comprehensive understanding of the relationships between urban environments, natural features, ad human well-being.

Furthermore, to improve the estimation of GVI for missing points using mean NDVI values, it is worth considering the inclusion of more variables, such as building density, height, and orientation. However, such building data are mostly unavailable globally, but more and more data on building are becoming available such as OSM building by Microsoft Building Footprints. Exploring these future research directions will not only expand upon the findings of this study but also contribute to the development of approaches for urban planning and public health interventions.

5. Conclusions

This research has developed and demonstrated a scalable, reproducible framework for utilising open-source and FAIR Mapillary image data to assess greenness visibility in diverse geographical contexts. Our achievement, readily accessible via the project's GitHub repository (Vázquez Sánchez & Labib, 2023), reaffirms the transparency and reliability of our work, serving as a valuable resource for researchers in need of reproducible methodologies.

Importantly, this research effectively addressed its research questions, demonstrating that despite variations in image availability across different cities, a robust methodology for GVI assessment can be established using images from Mapillary. Our study identified disparities in Mapillary data availability and usability across the selected global cities, bringing to light an uneven global distribution of open-source and free image data. Nonetheless, these disparities did not diminish the potential of Mapillary for GVI evaluations.

Additionally, our findings accentuate Mapillary's adherence to FAIR principles, an asset in scientific research in this domain. This feature makes Mapillary an advantageous free and FAIR alternative to Google Street View for GVI assessments despite the found discrepancies and temporal limitations that are not only inherent to crowdsourced data. Our methodology enables new avenues to make urban greenness analysis accessible to all.

A key innovation of our study was using globally available NDVI data to estimate GVI values at missing locations. Although not without limitations, this approach proved to be a promising method for augmenting street-level GVI analyses in data-scarce areas. The successful application of NDVI in our study paves the way for future research to refine and expand on this method, further enhancing the robustness of GVI analyses.

Additionally, this study provided a comparative analysis between cities of varying socio-economic contexts, finding a notable lesser greener visibility in densely populated, lower-income cities in South Asia and Africa as compared to their low-density, affluent counterparts in the USA and Europe.

Overall, this study serves as a critical contribution to the urban planning and environmental research, providing an accessible, scalable, and innovative approach to green view assessment. Our findings and established framework, founded on open-source data and reproducibility, facilitate comparative studies, and establish guidelines for green view assessments across the globe using free images. Through this, we hope to foster a greater understanding of the relationships between green urban environments and human well-being, driving toward a greener, healthier, and more equitable urban spaces.

6. References

Abebe, G. A. (2013). Quantifying urban growth pattern in developing countries using remote sensing and spatial metrics: A case study in Kampala, Uganda [University of Twente]. http://essay.utwente.nl/84729/1/abebe.pdf

Aguilar, A. G., & Lopez, F. M. (2018). The city-region of Mexico City: Social inequality and a vacuum in development planning. International Development Planning Review, 40(1), 51–74. https://doi.org/10.3828/idpr.2018.3

Aikoh, T., Homma, R., & Abe, Y. (2023). Comparing conventional manual measurement of the green view index with modern automatic methods using google street view and semantic segmentation. Urban Forestry & Urban Greening, 80, 127845. https://doi.org/10.1016/j.ufug.2023.127845

Akbari, H., Pomerantz, M., & Taha, H. (2001). Cool surfaces and shade trees to reduce energy use and improve air quality in urban areas. Solar Energy, 70(3), 295–310. https://doi.org/10.1016/S0038-092X(00)00089-X

Alonzo, M., Bookhagen, B., & Roberts, D. A. (2014). Urban tree species mapping using hyperspectral and lidar data fusion. Remote Sensing of Environment, 148, 70–83. https://doi.org/10.1016/j.rse.2014.03.018

Alvarez Leon, L. F., & Quinn, S. (2019). The value of crowdsourced street-level imagery: Examining the shifting property regimes of OpenStreetCam and Mapillary. GeoJournal, 84(2), 395–414. https://doi.org/10.1007/s10708-018-9865-4

Antequera, M. L., Gargallo, P., Hofinger, M., Bulò, S. R., Kuang, Y., & Kontschieder, P. (2020). Mapillary Planet-Scale Depth Dataset. In A. Vedaldi, H. Bischof, T. Brox, & J.-M. Frahm (Eds.), Computer Vision – ECCV 2020 (pp. 589–604). Springer International Publishing. https://doi.org/10.1007/978-3-030-58536-5_35

Armson, D., Stringer, P., & Ennos, A. R. (2013). The effect of street trees and amenity grass on urban surface water runoff in Manchester, UK. Urban Forestry & Urban Greening, 12(3), 282–286. https://doi.org/10.1016/j.ufug.2013.04.001

Attal, E., Dubus, B., Leblois, T., & Cretin, B. (2021). An optimal dimensioning method of a green wall structure for noise pollution reduction. Building and Environment, 187, 107362. https://doi.org/10.1016/j.buildenv.2020.107362

Bain, L., Gray, B., & Rodgers, D. (2012). Living Streets: Strategies for Crafting Public Space. John Wiley & Sons.

Batlle, J., Casals, A., Freixenet, J., & Martí, J. (2000). A review on strategies for recognizing natural objects in colour images of outdoor scenes. Image and Vision Computing, 18(6), 515–530. https://doi.org/10.1016/S0262-8856(99)00040-2

Berland, A., Shiflett, S. A., Shuster, W. D., Garmestani, A. S., Goddard, H. C., Herrmann, D. L., & Hopton, M. E. (2017). The role of trees in urban stormwater management. Landscape and Urban Planning, 162, 167–177. https://doi.org/10.1016/j.landurbplan.2017.02.017

Biljecki, F., & Ito, K. (2021). Street view imagery in urban analytics and GIS: A review. Landscape and Urban Planning, 215, 104217. https://doi.org/10.1016/j.landurbplan.2021.104217

Boeing, G. (2017). OSMnx: New methods for acquiring, constructing, analyzing, and visualizing complex street networks. Computers, Environment and Urban Systems, 65, 126–139. https://doi.org/10.1016/j.compenvurbsys.2017.05.004

Bush, J., Ashley, G., Foster, B., & Hall, G. (2021). Integrating Green Infrastructure into Urban Planning: Developing Melbourne's Green Factor Tool. Urban Planning, 6, 20–31. https://doi.org/10.17645/up.v6i1.3515

Cai, B. Y., Li, X., Seiferling, I., & Ratti, C. (2018, August 14). Treepedia 2.0: Applying Deep Learning for Large-scale Quantification of Urban Tree Cover. ArXiv.Org. https://doi.org/10.1109/bigdatacongress.2018.00014

Chen, J., Zhou, C., & Li, F. (2020). Quantifying the green view indicator for assessing urban greening quality: An analysis based on Internet-crawling street view data. Ecological Indicators, 113, 106192. https://doi.org/10.1016/j.ecolind.2020.106192

Chen, S., & Biljecki, F. (2023). Automatic assessment of public open spaces using street view imagery. Cities, 137, 104329. https://doi.org/10.1016/j.cities.2023.104329

Cheng, B., Misra, I., Schwing, A. G., Kirillov, A., & Girdhar, R. (2022). Masked-attention Mask Transformer for Universal Image Segmentation. 2022 IEEE/CVF Conference on Computer Vision and Pattern Recognition (CVPR), 1280–1289. https://doi.org/10.1109/CVPR52688.2022.00135

Corbane, C., Politis, P., Kempeneers, P., Simonetti, D., Soille, P., Burger, A., Pesaresi, M., Sabo, F., Syrris, V., & Kemper, T. (2020). A global cloud free pixel- based image composite from Sentinel-2 data. Data in Brief, 31, 105737. https://doi.org/10.1016/j.dib.2020.105737

D'Andrimont, R., Yordanov, M., Lemoine, G., Yoong, J., Nikel, K., & Van der Velde, M. (2018). Crowdsourced Street-Level Imagery as a Potential Source of In-Situ Data for Crop Monitoring. Land, 7(4), Article 4. https://doi.org/10.3390/land7040127

Dierwechter, Y. (2017). Urban Sustainability through smart growth: Intercurrence, planning, and geographies of regional development across Greater Seattle. Springer. https://link.springer.com/content/pdf/10.1007/978-3-319-54448-9.pdf

Dong, R., Zhang, Y., & Zhao, J. (2018). How Green Are the Streets Within the Sixth Ring Road of Beijing? An Analysis Based on Tencent Street View Pictures and the Green View Index. International Journal of Environmental Research and Public Health, 15(7), Article 7. https://doi.org/10.3390/ijerph15071367

Downs, R. M., & Stea, D. (1977). Maps in minds. Reflections on cognitive mapping.

Edson, C., & Wing, M. G. (2011). Airborne Light Detection and Ranging (LiDAR) for Individual Tree Stem Location, Height, and Biomass Measurements. Remote Sensing, 3(11), Article 11. https://doi.org/10.3390/rs3112494

Ellaway, A., Macintyre, S., & Bonnefoy, X. (2005). Graffiti, greenery, and obesity in adults: Secondary analysis of European cross sectional survey. BMJ, 331(7517), 611–612. https://doi.org/10.1136/bmj.38575.664549.F7

Falfán, I., Muñoz-Robles, C. A., Bonilla-Moheno, M., & MacGregor-Fors, I. (2018). Can you really see 'green'? Assessing physical and self-reported measurements of urban greenery. Urban Forestry & Urban Greening, 36, 13–21. https://doi.org/10.1016/j.ufug.2018.08.016

Fry, D., Mooney, S. J., Rodríguez, D. A., Caiaffa, W. T., & Lovasi, G. S. (2020). Assessing Google Street View Image Availability in Latin American Cities. Journal of Urban Health, 97(4), 552–560. https://doi.org/10.1007/s11524-019-00408-7

Gómez-Baggethun, E., & Barton, D. N. (2013). Classifying and valuing ecosystem services for urban planning. Ecological Economics, 86, 235–245. https://doi.org/10.1016/j.ecolecon.2012.08.019

Google. (2018a). Google Maps APIs Terms of Service. Google for Developers. https://developers.google.com/maps/terms-20180207?hl=es-419

Google. (2018b). Google Maps, Google Earth, and Street View. https://about.google/brand-resource-center/products-and-services/geo-guidelines/

Google. (2020). Google Maps Platform Terms Of Service. Google Cloud. https://cloud.google.com/maps-platform/terms

Google. (2023). Google Maps Platform Pricing. Google for Developers. https://developers.google.com/maps/billing-and-pricing/pricing

Gupta, K., Kumar, P., Pathan, S. K., & Sharma, K. P. (2012). Urban Neighborhood Green Index – A measure of green spaces in urban areas. Landscape and Urban Planning, 105(3), 325–335. https://doi.org/10.1016/j.landurbplan.2012.01.003

Hara, K., Le, V., & Froehlich, J. (2013). Combining crowdsourcing and google street view to identify street-level accessibility problems. Proceedings of the SIGCHI Conference on Human Factors in Computing Systems, 631–640. https://doi.org/10.1145/2470654.2470744

Helbich, M., Yao, Y., Liu, Y., Zhang, J., Liu, P., & Wang, R. (2019). Using deep learning to examine street view green and blue spaces and their associations with geriatric depression in Beijing, China. Environment International, 126, 107–117. https://doi.org/10.1016/j.envint.2019.02.013

Herscovici, A., Dahan, G., & Cohen, G. (2022). Smart Cities and Tourism: The Case of Tel Aviv-Yafo. Sustainability, 14(17), Article 17. https://doi.org/10.3390/su141710968

Inoue, T., Manabe, R., Murayama, A., & Koizumi, H. (2022). Landscape value in urban neighborhoods: A pilot analysis using street-level images. Landscape and Urban Planning, 221, 104357. https://doi.org/10.1016/j.landurbplan.2022.104357

Jim, C. Y., & Chen, W. Y. (2008). Assessing the ecosystem service of air pollutant removal by urban trees in Guangzhou (China). Journal of Environmental Management, 88(4), 665–676. https://doi.org/10.1016/j.jenvman.2007.03.035

Jimenez, M. P., Suel, E., Rifas-Shiman, S. L., Hystad, P., Larkin, A., Hankey, S., Just, A. C., Redline, S., Oken, E., James, P., & See Acknowledgments for full listing of collaborators. (2022). Street-view greenspace exposure and objective sleep characteristics among children. Environmental Research, 214(Pt 1), 113744. https://doi.org/10.1016/j.envres.2022.113744

Juhász, L., & Hochmair, H. H. (2016). User Contribution Patterns and Completeness Evaluation of Mapillary, a Crowdsourced Street Level Photo Service. Transactions in GIS, 20(6), 925–947. https://doi.org/10.1111/tgis.12190

Kaplan, S. (1995). The restorative benefits of nature: Toward an integrative framework. Journal of Environmental Psychology, 15(3), 169–182. https://doi.org/10.1016/0272-4944(95)90001-2

Keeley, M. (2011). The Green Area Ratio: An urban site sustainability metric. Journal of Environmental Planning and Management, 54(7), 937–958. https://doi.org/10.1080/09640568.2010.547681

Ki, D., & Lee, S. (2021). Analyzing the effects of Green View Index of neighborhood streets on walking time using Google Street View and deep learning. Landscape and Urban Planning, 205, 103920. https://doi.org/10.1016/j.landurbplan.2020.103920

Kido, D., Fukuda, T., & Yabuki, N. (2021). Assessing future landscapes using enhanced mixed reality with semantic segmentation by deep learning. Advanced Engineering Informatics, 48, 101281. https://doi.org/10.1016/j.aei.2021.101281

Krylov, V. A., & Dahyot, R. (2019). Object Geolocation from Crowdsourced Street Level Imagery. In C. Alzate, A. Monreale, H. Assem, A. Bifet, T. S. Buda, B. Caglayan, B. Drury, E. García-Martín, R. Gavaldà, I. Koprinska, S. Kramer, N. Lavesson, M. Madden, I. Molloy, M.-I. Nicolae, & M. Sinn (Eds.), ECML PKDD 2018 Workshops (pp. 79–83). Springer International Publishing. https://doi.org/10.1007/978-3-030-13453-2_7

Labib, S. M., Huck, J. J., & Lindley, S. (2021). Modelling and mapping eye-level greenness visibility exposure using multi-source data at high spatial resolutions. Science of The Total Environment, 755, 143050. https://doi.org/10.1016/j.scitotenv.2020.143050

Labib, S. M., Lindley, S., & Huck, J. J. (2020). Spatial dimensions of the influence of urban green-blue spaces on human health: A systematic review. Environmental Research, 180, 108869. https://doi.org/10.1016/j.envres.2019.108869

Lafortezza, R., Carrus, G., Sanesi, G., & Davies, C. (2009). Benefits and well-being perceived by people visiting green spaces in periods of heat stress. Urban Forestry & Urban Greening, 8(2), 97–108. https://doi.org/10.1016/j.ufug.2009.02.003

Larkin, A., & Hystad, P. (2019). Evaluating street view exposure measures of visible green space for health research. Journal of Exposure Science & Environmental Epidemiology, 29(4), Article 4. https://doi.org/10.1038/s41370-018-0017-1

Li, X., Zhang, C., Li, W., Kuzovkina, Y. A., & Weiner, D. (2015). Who lives in greener neighborhoods? The distribution of street greenery and its association with residents' socioeconomic conditions in Hartford, Connecticut, USA. Urban Forestry & Urban Greening, 14(4), 751–759. https://doi.org/10.1016/j.ufug.2015.07.006

Li, X., Zhang, C., Li, W., Ricard, R., Meng, Q., & Zhang, W. (2015). Assessing street-level urban greenery using Google Street View and a modified green view index. Urban Forestry & Urban Greening, 14(3), 675–685. https://doi.org/10.1016/j.ufug.2015.06.006

Liang, Y., D'Uva, D., Scandiffio, A., & Rolando, A. (2022). The more walkable, the more livable? -- Can urban attractiveness improve urban vitality? Transportation Research Procedia, 60, 322–329. https://doi.org/10.1016/j.trpro.2021.12.042

Lindemann-Matthies, P., & Brieger, H. (2016). Does urban gardening increase aesthetic quality of urban areas? A case study from Germany. Urban Forestry & Urban Greening, 17, 33–41. https://doi.org/10.1016/j.ufug.2016.03.010

Long, Y., & Liu, L. (2017). How green are the streets? An analysis for central areas of Chinese cities using Tencent Street View. PLOS ONE, 12(2), e0171110. https://doi.org/10.1371/journal.pone.0171110

Lu, Y. (2019). Using Google Street View to investigate the association between street greenery and physical activity. Landscape and Urban Planning, 191, 103435. https://doi.org/10.1016/j.landurbplan.2018.08.029

Lu, Y., Ferranti, E. J. S., Chapman, L., & Pfrang, C. (2023). Assessing urban greenery by harvesting street view data: A review. Urban Forestry & Urban Greening, 83, 127917. https://doi.org/10.1016/j.ufug.2023.127917

Lu, Y., Sarkar, C., & Xiao, Y. (2018). The effect of street-level greenery on walking behavior: Evidence from Hong Kong. Social Science & Medicine, 208, 41–49. https://doi.org/10.1016/j.socscimed.2018.05.022

Ma, D., Fan, H., Li, W., & Ding, X. (2020). The State of Mapillary: An Exploratory Analysis. ISPRS International Journal of Geo-Information, 9(1), Article 1. https://doi.org/10.3390/ijgi9010010

Mapbox. (2023). Vector tiles standards (Tilesets). Mapbox. https://docs.mapbox.com/data/tilesets/guides/vector-tiles-standards/

Mapillary. (2021, June 21). Mapillary API Documentation. https://www.mapillary.com/developer/api-documentation?locale=es_ES

Martinez, A. de la I., & Labib, S. M. (2023). Demystifying normalized difference vegetation index (NDVI) for greenness exposure assessments and policy interventions in urban greening. Environmental Research, 220, 115155. https://doi.org/10.1016/j.envres.2022.115155

Meitner, M. J. (2004). Scenic beauty of river views in the Grand Canyon: Relating perceptual judgments to locations. Landscape and Urban Planning, 68(1), 3–13. https://doi.org/10.1016/S0169-2046(03)00115-4

Meraner, A., Ebel, P., Zhu, X., & Schmitt, M. (2020). Cloud Removal in Sentinel-2 Imagery using a Deep Residual Neural Network and SAR-Optical Data Fusion. ISPRS Journal of Photogrammetry and Remote Sensing, 166, 333–346. https://doi.org/10.1016/j.isprsjprs.2020.05.013

MIT Senseable City Lab. (2023). Treepedia. Treepedia: MIT Senseable City Lab. http://senseable.mit.edu/treepedia

Mora, L., & Bolici, R. (2017). How to Become a Smart City: Learning from Amsterdam. In A. Bisello, D. Vettorato, R. Stephens, & P. Elisei (Eds.), Smart and Sustainable Planning for Cities and Regions: Results of SSPCR 2015 (pp. 251–266). Springer International Publishing. https://doi.org/10.1007/978-3-319-44899-2_15

Mortoja, M. G., & Yigitcanlar, T. (2022). Factors influencing peri-urban growth: Empirical evidence from the Dhaka and Brisbane regions. Remote Sensing Applications: Society and Environment, 26, 100762. https://doi.org/10.1016/j.rsase.2022.100762

Nielsen, J. (2006, October 8). The 90-9-1 Rule for Participation Inequality in Social Media and Online Communities. Nielsen Norman Group. https://www.nngroup.com/articles/participation-inequality/

Ordóñez, C., Labib, S. M., Chung, L., & Conway, T. M. (2023). Satisfaction with urban trees associates with tree canopy cover and tree visibility around the home. Npj Urban Sustainability, 3(1), Article 1. https://doi.org/10.1038/s42949-023-00119-8

O'Regan, A. C., Byrne, R., Hellebust, S., & Nyhan, M. M. (2022). Associations between Google Street View-derived urban greenspace metrics and air pollution measured using a distributed sensor network. Sustainable Cities and Society, 87, 104221. https://doi.org/10.1016/j.scs.2022.104221

Pietikainen, M., Nieminen, S., Marszalec, E., & Ojala, T. (1996). Accurate color discrimination with classification based on feature distributions. Proceedings of 13th International Conference on Pattern Recognition, 3, 833–838 vol.3. https://doi.org/10.1109/ICPR.1996.547285

Rangel, J. C., Cruz, E., & Cazorla, M. (2022). Automatic Understanding and Mapping of Regions in Cities Using Google Street View Images. Applied Sciences, 12(6), Article 6. https://doi.org/10.3390/app12062971

Root, E. D., Silbernagel, K., & Litt, J. S. (2017). Unpacking healthy landscapes: Empirical assessment of neighborhood aesthetic ratings in an urban setting. Landscape and Urban Planning, 168, 38–47. https://doi.org/10.1016/j.landurbplan.2017.09.028

Rundle, A. G., Bader, M. D. M., & Mooney, S. J. (2022). Machine Learning Approaches for Measuring Neighborhood Environments in Epidemiologic Studies. Current Epidemiology Reports, 9(3), 175–182. https://doi.org/10.1007/s40471-022-00296-7

Rzotkiewicz, A., Pearson, A. L., Dougherty, B. V., Shortridge, A., & Wilson, N. (2018). Systematic review of the use of Google Street View in health research: Major themes, strengths, weaknesses and possibilities for future research. Health & Place, 52, 240–246. https://doi.org/10.1016/j.healthplace.2018.07.001

Satellite Imaging Corporation. (2022). Sentinel-2A SatelliteSensor. https://www.satimagingcorp.com/satellite-sensors/other-satellite-sensors/sentinel-2a/

Savo, V., D'Amato, L., Bartoli, F., Zappitelli, I., & Caneva, G. (2023). Trees are Not All the Same: Evaluation of Main Regulating, Provision, and Supporting Ecosystem Services of Urban Street Trees (SSRN Scholarly Paper No. 4470051). https://doi.org/10.2139/ssrn.4470051

Saw, L. E., Lim, F. K. S., & Carrasco, L. R. (2015). The Relationship between Natural Park Usage and Happiness Does Not Hold in a Tropical City-State. PLOS ONE, 10(7), e0133781. https://doi.org/10.1371/journal.pone.0133781

SciPy. (2022, July 29). SciPy Documentation. https://docs.scipy.org/doc/scipy-1.9.0/

Seiferling, I., Naik, N., Ratti, C., & Proulx, R. (2017). Green streets − Quantifying and mapping urban trees with street-level imagery and computer vision. Landscape and Urban Planning, 165, 93–101. https://doi.org/10.1016/j.landurbplan.2017.05.010

Shrestha, R., & Wynne, R. H. (2012). Estimating Biophysical Parameters of Individual Trees in an Urban Environment Using Small Footprint Discrete-Return Imaging Lidar. Remote Sensing, 4(2), Article 2. https://doi.org/10.3390/rs4020484

Stringam, B., Gerdes, J. H., & Anderson, C. K. (2023). Legal and Ethical Issues of Collecting and Using Online Hospitality Data. Cornell Hospitality Quarterly, 64(1), 54–62. https://doi.org/10.1177/19389655211040434

Suppakittpaisarn, P., Lu, Y., Jiang, B., & Slavenas, M. (2022). How do computers see landscapes? Comparisons of eye-level greenery assessments between computer and human perceptions. Landscape and Urban Planning, 227, 104547. https://doi.org/10.1016/j.landurbplan.2022.104547

Tang, J., & Long, Y. (2019). Measuring visual quality of street space and its temporal variation: Methodology and its application in the Hutong area in Beijing. Landscape and Urban Planning, 191, 103436. https://doi.org/10.1016/j.landurbplan.2018.09.015

Torkko, J., Poom, A., Willberg, E., & Toivonen, T. (2023). How to best map greenery from a human perspective? Comparing computational measurements with human perception. Frontiers in Sustainable Cities, 5. https://www.frontiersin.org/articles/10.3389/frsc.2023.1160995

Ulrich, R. S. (1984). View Through a Window May Influence Recovery from Surgery. Science, 224(4647), 420–421. https://doi.org/10.1126/science.6143402

United Nations. (2018). World Urbanizaton Prospects 2018. United Nations Department of Economic and Social Affairs.

Vázquez Sánchez, I. A., & Labib, S. (2023). Automated Green View Index Modeling Pipeline using Mapillary Street Images and Transformer models. Zenodo. https://doi.org/10.5281/zenodo.8106479

Wang, R., Browning, M. H. E. M., Qin, X., He, J., Wu, W., Yao, Y., & Liu, Y. (2022). Visible green space predicts emotion: Evidence from social media and street view data. Applied Geography, 148, 102803. https://doi.org/10.1016/j.apgeog.2022.102803

Wilkinson, M. D., Dumontier, M., Aalbersberg, Ij. J., Appleton, G., Axton, M., Baak, A., Blomberg, N., Boiten, J.-W., da Silva Santos, L. B., Bourne, P. E., Bouwman, J., Brookes, A. J., Clark, T., Crosas, M., Dillo, I., Dumon, O., Edmunds, S., Evelo, C. T., Finkers, R., … Mons, B. (2016). The FAIR Guiding Principles for scientific data management and stewardship. Scientific Data, 3(1), Article 1. https://doi.org/10.1038/sdata.2016.18

Wolf, K. L. (2005). Business District Streetscapes, Trees, and Consumer Response. Journal of Forestry, 103(8), 396–400. https://doi.org/10.1093/jof/103.8.396

Wong, N. H., Kwang Tan, A. Y., Tan, P. Y., Chiang, K., & Wong, N. C. (2010). Acoustics evaluation of vertical greenery systems for building walls. Building and Environment, 45(2), 411–420. https://doi.org/10.1016/j.buildenv.2009.06.017

Xia, Y., Yabuki, N., & Fukuda, T. (2021). Development of a system for assessing the quality of urban street-level greenery using street view images and deep learning. Urban Forestry & Urban Greening, 59, 126995. https://doi.org/10.1016/j.ufug.2021.126995

Yang, J., Kang, Z., Cheng, S., Yang, Z., & Akwensi, P. H. (2020). An Individual Tree Segmentation Method Based on Watershed Algorithm and Three-Dimensional Spatial Distribution Analysis From Airborne LiDAR Point Clouds. IEEE Journal of Selected Topics in Applied Earth Observations and Remote Sensing, 13, 1055–1067. https://doi.org/10.1109/JSTARS.2020.2979369

Yang, J., Zhao, L., Mcbride, J., & Gong, P. (2009). Can you see green? Assessing the visibility of urban forests in cities. Landscape and Urban Planning, 91(2), 97–104. https://doi.org/10.1016/j.landurbplan.2008.12.004

Yao, Y., Zhu, X., Xu, Y., Yang, H., Wu, X., Li, Y., & Zhang, Y. (2012). Assessing the visual quality of green landscaping in rural residential areas: The case of Changzhou, China. Environmental Monitoring and Assessment, 184(2), 951–967. https://doi.org/10.1007/s10661-011-2012-z

Yap, W., Chang, J.-H., & Biljecki, F. (2022). Incorporating networks in semantic understanding of streetscapes: Contextualising active mobility decisions. Environment and Planning B: Urban Analytics and City Science, 23998083221138830. https://doi.org/10.1177/23998083221138832

Ye, Y., Richards, D., Lu, Y., Song, X., Zhuang, Y., Zeng, W., & Zhong, T. (2019). Measuring daily accessed street greenery: A human-scale approach for informing better urban planning practices. Landscape and Urban Planning, 191, 103434. https://doi.org/10.1016/j.landurbplan.2018.08.028

Yu, S., Yu, B., Song, W., Wu, B., Zhou, J., Huang, Y., Wu, J., Zhao, F., & Mao, W. (2016). View-based greenery: A three-dimensional assessment of city buildings' green visibility using Floor Green View Index. Landscape and Urban Planning, 152, 13–26. https://doi.org/10.1016/j.landurbplan.2016.04.004

Yu, X., Zhao, G., Chang, C., Yuan, X., & Heng, F. (2019). BGVI: A New Index to Estimate Street-Side Greenery Using Baidu Street View Image. Forests, 10(1), Article 1. https://doi.org/10.3390/f10010003

Zheng, X., & Amemiya, M. (2023). Method for Applying Crowdsourced Street-Level Imagery Data to Evaluate Street-Level Greenness. ISPRS International Journal of Geo-Information, 12(3), Article 3. https://doi.org/10.3390/ijgi12030108

Zijlema, W. L., Triguero-Mas, M., Cirach, M., Gidlow, C., Kruize, H., Grazuleviciene, R., Nieuwenhuijsen, M. J., & Litt, J. S. (2020). Understanding correlates of neighborhood aesthetic ratings: A European-based Four City comparison. Urban Forestry & Urban Greening, 47, 126523. https://doi.org/10.1016/j.ufug.2019.126523